

This article was downloaded by:

On: 21 January 2011

Access details: *Access Details: Free Access*

Publisher *Taylor & Francis*

Informa Ltd Registered in England and Wales Registered Number: 1072954 Registered office: Mortimer House, 37-41 Mortimer Street, London W1T 3JH, UK



The Journal of Adhesion

Publication details, including instructions for authors and subscription information:

<http://www.informaworld.com/smpp/title~content=t713453635>

An Investigation of Interfacial Stresses in Reinforced Concrete Beams Using FRP Laminates

Baris Sayin^a; Ekrem Manisali^b

^a Construction Works & Technical Department, Istanbul University, Istanbul, Turkey ^b Department of Civil Engineering, Faculty of Engineering, Istanbul University, Istanbul, Turkey

Online publication date: 09 November 2010

To cite this Article Sayin, Baris and Manisali, Ekrem(2010) 'An Investigation of Interfacial Stresses in Reinforced Concrete Beams Using FRP Laminates', *The Journal of Adhesion*, 86: 11, 1132 – 1157

To link to this Article: DOI: 10.1080/00218464.2010.519260

URL: <http://dx.doi.org/10.1080/00218464.2010.519260>

PLEASE SCROLL DOWN FOR ARTICLE

Full terms and conditions of use: <http://www.informaworld.com/terms-and-conditions-of-access.pdf>

This article may be used for research, teaching and private study purposes. Any substantial or systematic reproduction, re-distribution, re-selling, loan or sub-licensing, systematic supply or distribution in any form to anyone is expressly forbidden.

The publisher does not give any warranty express or implied or make any representation that the contents will be complete or accurate or up to date. The accuracy of any instructions, formulae and drug doses should be independently verified with primary sources. The publisher shall not be liable for any loss, actions, claims, proceedings, demand or costs or damages whatsoever or howsoever caused arising directly or indirectly in connection with or arising out of the use of this material.

An Investigation of Interfacial Stresses in Reinforced Concrete Beams Using FRP Laminates

Baris Sayin¹ and Ekrem Manisali²

¹Construction Works & Technical Department, Istanbul University, Istanbul, Turkey

²Department of Civil Engineering, Faculty of Engineering, Istanbul University, Istanbul, Turkey

Reinforcement of reinforced concrete (RC) beams against bending through utilization of bonded fibre-reinforced plastic (FRP) laminates has been accepted as an effective method of strengthening. In this study, the effects of FRP reinforcement over the parameters of interfacial stresses in reinforced concrete beams were examined both experimentally and numerically. Essentially, the main goal of the study was to investigate quantitatively the behaviour of the RC beams strengthened with adhesively bonded FRP. In order to achieve this goal, an experimental study was initially carried out. Afterwards, the ANSYS[®] WB finite element program was employed to model and analyze the RC beams externally bonded to FRP. The obtained results are expected to demonstrate the main characteristics of interfacial stress distributions inside beams strengthened with FRP. The evaluation of interfacial stresses provides the basis for understanding the main characteristics in such beams and for developing suitable design rules.

Keywords: Adhesive; Fibre reinforced plastic (FRP); Finite element analysis; Interfacial stresses; Reinforced concrete (RC) beam

1. INTRODUCTION

For more than 15 years, strengthening of reinforced concrete (RC) beams in flexure by adhesive bonding of a fibre reinforced plastic (FRP) laminate to the tension face has become an accepted and general method due to the favourable mechanical properties of FRP composites. Externally bonded FRP reinforcement has been shown to

Received 7 December 2009; in final form 20 July 2010.

Address correspondence to Baris Sayin, Construction Works & Technical Department, Istanbul University, Fatih, Istanbul 34116, Turkey. E-mail: barsayin@istanbul.edu.tr

be applicable for the strengthening of many types of RC structures such as columns, beams, slabs, walls, tunnels, and silos. It can also be used to improve flexural and shear capacities and provide confinement and ductility to compression members [1,2]. Considering FRP's superior properties, such as increasing the strength and stiffness of an existing beam, long-term durability, corrosion resistance, light weight and easy installation, this technique exhibits many advantages in comparison with traditional ones. However, on the whole, the strengthening method displays certain disadvantages, including the reduction of the strengthened member's ductility and the rotating capability of the strengthened section. In the flexural strengthening method, the FRP reinforcement can be externally bonded to the tension face of the members with fibers oriented along the length of the member to increase the entire performance of strengthened RC beams. Although strong bonding at the interface is essential for the efficient transfer of stress, it generally leads to unstable catastrophic failure, as a consequence of cracks propagating right through the reinforcement (transverse cracking) and with very limited energy absorption capacity. In contrast, weak interface bonding allows the toughening mechanisms to take place more extensively through longitudinal splitting. Therefore, the capacity of load transfer will be reduced and a longer concrete crack spacing and crack width will ensue [4]. Within this scope, adhesive layer thickness, adhesive layer type, characteristics of the concrete surface, and stress transfer are important during FRP application. These parameters modify the load bearing capacity, load-deflection relationships, debonding at the end of the bonded FRP, and the normal and shear stress concentrations between FRP and concrete.

A number of researches [5–26] have been carried out to investigate the behaviour of beams with FRP laminates with respect to reinforcement in bending; *e.g.*, the study by Yang *et al.* [13], who studied the stress transfer in concrete beams bonded with FRP plates. They reported that a novel simplified interfacial stress formulation for the FRP bonded concrete beams that had been subjected to arbitrary loadings. They concluded that this formulation could easily be incorporated into the strength models to predict debonding loads.

A numerical model that can be used for the assessment of retrofitting and repair systems based on the employment of FRP in reinforced concrete columns and beams was reported by Rougier and Luccioni [14]. The presented model accurately reproduces the behaviour of confined concrete, not only in the axial direction, but also in the transverse one, as well as the response of flexural concrete members. Finally, the model was also capable of reproducing the shear and crushing failure of the concrete.

Gheorghiu *et al.* [15] conducted an experimental project in order to assess the durability of RC beams strengthened with carbon-fibre-reinforced polymers (CFRPs). Load-deflection curves and strain responses provide an insight into the performance of CFRP-strengthened beams subjected to severe loading conditions.

Rabinovitch [16] analytically studied the bending behaviour of reinforced concrete beams strengthened with composite materials externally bonded with nonlinear and inelastic adhesives. The results imply that the usage of such adhesive materials improves the overall load carrying behavior of the strengthened beam, increases its ductility, provides the mechanism for the formation of plastic hinges, and reduces the shear stresses near the ends of the bonded strip.

Masoud and Soudki [17] carried out an experimental study to evaluate the corrosion activity in reinforced concrete beams repaired with fibre reinforced polymer (FRP) sheets. They reported that their experimental results demonstrated a decrease in the corrosion potential as corrosion progressed, and the FRP repair led to a larger drop in the corrosion potential with time than that observed without any FRP application. The results showed that the mass loss of the main reinforcing bars due to corrosion was reduced by up to 16% by virtue of FRP repair.

Teng *et al.* [18] studied an analytical solution for the debonding process in an FRP-to-concrete bonded joint model where the FRP plate was subjected to tension at both ends. The expressions for the interfacial shear stress distribution and the load-displacement response were derived for different loading stages. While the emphasis of the paper was on FRP-to-concrete joints, the analytical solution was equally applicable to similar joints between thin plates of other materials (*e.g.*, steel and aluminium) and concrete.

Gao *et al.* [19] examined a simple and accurate design methodology to predict the load carrying capacity of a strengthened RC beam when concrete cover separation takes place. An analytical expression was developed by taking into account the stress concentrations in concrete near the tension rebar closest to the cut-off point of the FRP strip. The predictions based on the present analytical model were compared with the 58 different sets of experimental data found in the literature and observed to be in good agreement. The expressions derived in the study, therefore, have the potential for application in the design of FRP-strengthened beams.

Jianzhuang *et al.* [20] studied the bond behaviour between FRP and concrete with two kinds of tests. Based on the test results, conclusions were made, such as the maximum effective bond length, the mean bond stress, and the region where bond stresses concentrate.

Chen and Teng [21] studied the development of a simple, accurate, and rational design proposal for the shear capacity of FRP-strengthened beams whose failure may occur as a result of FRP debonding. Existing strength proposals were reviewed and their deficiencies were highlighted. A new strength model was developed, which was validated by the experimental data collected from the existing literature. Finally, a new design proposal was presented.

Pesic and Pilakoutas [22] studied the problem of early concrete cover delamination and plate-end failure of reinforced concrete beams strengthened with externally bonded FRP-reinforcement. Two distinct design approaches based on the maximum tensile strength and shear capacity of concrete beams were initially examined, and it was found that linear elastic analysis cannot accurately predict the brittle plate-end concrete failure. It was also observed that the extent of achievable strengthening is limited by the shear capacity of concrete beams. The FE analysis was used to examine the effects of internal tensile reinforcement on the magnitude of principal tensile stresses in the critical region. Finally, the mixed mode of failure due to the combined effects of shear and concrete cover delamination was addressed by modelling the plate-end and shear crack discontinuities using the discrete crack approach.

Smith and Teng [23] started with a review of approximate closed-form solutions for interfacial stresses, followed by identifying their assumptions and limitations, thereby clarifying the differences between these solutions. This review also establishes the need for a similar, yet more accurate solution, and such a solution is presented in the paper. This new solution was intended for application to beams made of all kinds of materials bonded with a thin plate, whereas all of the existing solutions had been developed focusing on the strengthening of RC beams, which in turn allowed the omission of certain terms. Finally, numerical comparisons between the existing solutions and the current new solution have enabled a clear appreciation of the effects of various parameters.

Khalifa and Nanni [24] investigated the shear performance of RC beams with T-sections. Different configurations of externally bonded carbon fiber-reinforced polymer (CFRP) sheets were used to strengthen the specimens against shear. The experimental program consisted of six full-scale, simply supported beams. One of the beams was used as a benchmark and the remaining five beams were strengthened using different configurations of CFRP. The experimental results showed that the usage of externally bonded CFRP can increase the shear capacity of the beam significantly. In addition,

the results indicated that the most effective configuration was the U-wrap with end anchorage.

Alsayed [25] reported the results of the comparison conducted between the predicted and measured load-deflection relationships for 12 concrete beams reinforced with either steel or glass fibre reinforced plastic (GFRP) bars. The numerical part of the study was carried out using the following models: (i) the computer model which accounts for the actual properties of the composite constituents developed as part of this study, (ii) the ACI load-deflection model, and finally (iii) the modified load-deflection model available in the literature for beams reinforced by FRP bars. The computer model provides an accurate prediction of the measured service and full load-deflection curves. The error levels in the prediction of service load deflection and ultimate flexural strength are less than 10 and 1%, respectively. In the case of GFRP reinforced beams, the service load deflection predicted by the ACI model is in error by 70%, while that predicted by the modified model is in error by less than 15%.

Tounsi and Benyoucef [26] developed an analytical method to predict the distributions of interfacial stresses in concrete beams strengthened with composite plates. Accurate prediction of such stresses is a prerequisite to come up with the designs to prevent debonding failures of the FRP plate from the RC beam. In the present analysis, a simple theoretical model to estimate shear and peel-off stresses has been proposed, including the variation in FRP plate fibre orientation. Numerical results from the proposed analysis have been exhibited both to demonstrate the advantages of the present solution over existing ones and to illustrate the main characteristics of interfacial stress distributions in the beams.

In the light of the above explanation, the correct modelling of the FRP-to-concrete interface is the key step for accurate prediction of the interfacial stresses of RC beams strengthened with FRP. This study presents the results of the obtained stress values and load bearing capacities for 14 samples of RC beams reinforced by fibre reinforced plastic laminates. Experimental and finite element analyses were used to investigate the above-mentioned parameters of RC beams strengthened by composite laminates. The proposed experimental and numerical studies focus on the adhesive layer, adhesive thickness, stress transfer characteristics, and concrete surface. Within this scope, the main goal of this study is to demonstrate the main characteristics of interfacial stress distributions in RC beams strengthened with FRP bonded adhesives. In order to achieve this goal, an experimental study was carried out at first and then the numerical analysis results were obtained.

2. MATERIALS AND METHODS

2.1. Experimental Program

Tests were conducted in the Construction-Materials Laboratory of the Civil Engineering Department at Istanbul University. All the beams, which have a total length of 750 and 600 mm between supports, were cast outside the laboratory. Test beam specimens were constructed in a size of $150 \times 150 \times 750$ mm. Portland cement (CEM I 42.5 R) was used in all the mixtures and calcareous aggregate was used as an aggregate material in this study. In the experimental study, a square cross-section with simply supported RC beams, which were strengthened with fiber reinforced polymer, was selected. Monotonic loading referring to the loading of four points, which were automatically controlled by a 300-kN capacity hydraulic jack, was applied and measured by a load cell. Fifteen RC beam specimens were tested during the study among these beams; beam B15 was the control beam, without additional FRP strengthening, while all the other beams were strengthened with FRP. The transverse steel rebars consisted of 8 mm diameter at 100 mm spacing and the longitudinal steel rebars consisted of 10 mm diameter with a yielding strength of 420 MPa. The specimens were designed as per Eurocode 2 [27].

The carbon fiber reinforced polymer (FRP) composite employed in this study was manufactured by Sika Corporation (Sika[®] Carbo-Dur[®] S1012, Sika Corporation, Istanbul, Turkey) which is a high strength, unidirectional carbon fiber. This laminate has a width of 100 mm and a thickness of 1.2 mm, and is field applied with Sikadur[®]-30 (Sika) and Sikadur-52 (Sika) epoxy to form a carbon fiber reinforced polymer system. Sikadur-30 is a solvent-free, thixotropic, structural two-part adhesive for bonding reinforcement, based on a combination of epoxy resins. Sikadur-52 injection resin is a solvent-free, super-low viscosity, two-component, moisture-insensitive epoxy resin system. In this study, only the bending effect was addressed and all measurements were determined by a two-point load application. To measure deflection, linear variable displacement transducers (LVDT) were used in the mid-span of beams and potential collapse of the supports was neglected. After the specimens were set up, all the beams were tested under four-point bending in the structural testing frame. The specimens were spanned 600 mm and loaded symmetrically about their centerline at two points, which were 200 mm apart. Two point value of load was applied and the computer controlled measures were monitored. A flexural frame, whose width, length and height are 840, 845, and 1215 mm, respectively, can be seen in Fig. 1.

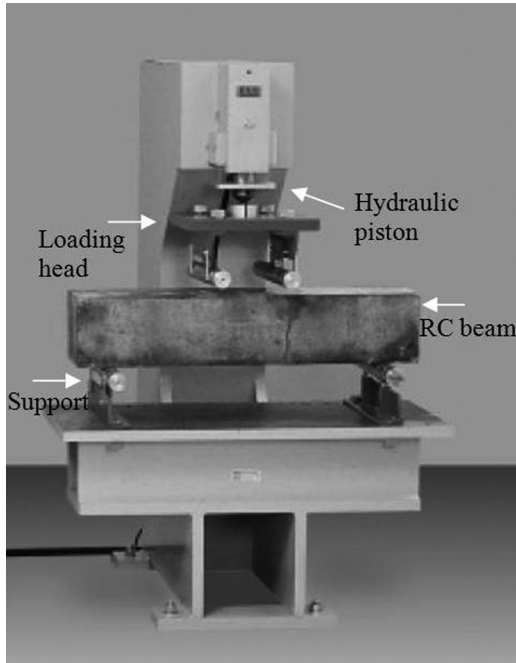


FIGURE 1 Photograph of experimental setup and instrumentation of beam (flexural frame).

Reinforced concrete beams were prepared under suitable conditions. Firstly, 15 specimens of steel rebars were prepared and concrete was produced by a ready-mixed concrete plant. Following that, the production of RC beams in steel formworks was conducted. For that, the steels were placed in formworks, consisting of box sections, and the steel rebars were placed inside the formwork. It is crucial for the concrete to have a smooth surface, since its lower surface would be exposed to adhesive. For achieving a smooth surface, the tension face of the reinforced concrete (RC) beam was sand-blasted and the dust particles were removed by using a wet sponge. Specimen dimensions were fixed according to the loading frame dimensions. The dimensions of all test beam specimens were set to consider this situation.

The compressive strength of concretes was determined on cube concrete molds which are $200 \times 200 \times 200$ mm in size. Twenty-four hours after concrete was placed in the cubic concrete mold, it was taken to the pool with water and cured where it would stay at a temperature of 21°C for 28 days. During the beam production process, two cube

samples were kept in the same conditions as the beams in the pool, and the strength of the beams were determined according to results of 7-day and 28-day compressive strength tests. According to the results of the cube samples, strength classes have been observed as C25, C30, and C35. The classification of concrete (*e.g.*, C20/25) refers to cylinder/cube strength as defined in Eurocode 2 Standard [27]. The sample strength values of the corresponding strength classes are given in Table 1. The samples exhibited compressive strength values of 25–35 MPa for 28 days. Geometry and loading of RC beams with FRP is given in Fig. 2.

The elastic modulus of the adhesive has not been mentioned in many studies. In these studies, the elastic modulus was assumed to be 8500 MPa, which is nearly equal to the average of the values reported for the other cases in the database (an average of 8697 MPa from 37 tests) [28]. The FRP and adhesive material properties which were used in this study are given in Tables 2 and 3.

Thickness values are smaller than 1, 2, and 4 mm of adhesive and dry/moist conditions of the concrete were tested. A and B components of the adhesive Sikadur[®]-30 were mixed in the ratio of 5:1. The moist condition was obtained by immersing the RC beams completely in water for 24 hours under laboratory conditions. A properly moistened sample under the conditions mentioned above was subjected to the epoxy adhesive application. For the polymerization of epoxy adhesives the RC beams were kept under the laboratory conditions for 1 week, and then they were examined in a four-point flexural test. The surface of the FRP was cleaned to remove any sign of dust. Since the reinforced concrete beams are produced in steel moulds no cleaning operation is needed before FRP laminates are applied to the beam.

The epoxy resin was mixed by an electrical mixer for 30 minutes until it turned to gray in colour. Steel wires (having diameters less than 1, 2, and 4 mm, according to the adhesive used), were placed on the beam to control the thickness of the adhesive. The adhesive (a paste) was then troweled into position on the surface of the concrete specimen and the FRP, previously cut to the required dimensions, was placed on the adhesive. A steel plate 70 × 15 × 3 cm (the “press tool”) was then placed on top of the FRP and kept there for 24 hours to provide pressure during the hardening of the epoxy resin.

The other adhesive, Sikadur 52, was quite fluid, and required a somewhat different application procedure. Steel wires were placed on the concrete beam to determine the thickness of the adhesive and the FRP laminate was put in place. Three edges of the assembly were sealed with steel plates (15 × 1 × 1 cm and 75 × 1 × 1 cm corresponding to the short and long edges of the laminate, respectively) and the beam was

TABLE 1 Cube Strength Values of Samples and Specified Strength Classes

Sample no	Slump (mm)	Count of sample	Day 7 Sample test values (MPa)	Day 28 Sample test values (MPa)	Coefficient of variation (%)	The strength classes according to the sample compressive strengths
B01	140	3	39	37	5.51	C30
B02						
B03	140	3	38	44	4.99	C30
B04						
B05	160	3	36	41	3.36	C30
B06						
B07	100	3	44	50	2.88	C35
B08						
B09	150	3	37	43	1.66	C30
B10						
B11	190	4	26	32	2.24	C25
B12						
B13	110	4	39	45	4.56	C35
B14						
B15	180	4	32	34	4.04	C30
—						

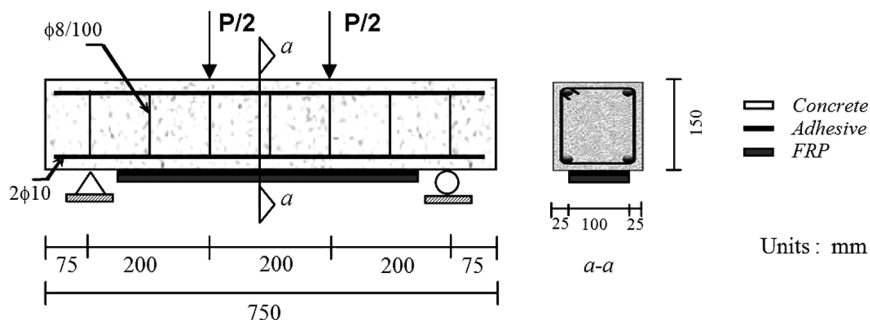


FIGURE 2 Loading, boundary conditions, and geometric dimensions of reinforced concrete (RC) beam with FRP.

fixed at an angle of 45° so that the open edge was at the top. Sikadur 52 was then injected into the space between the laminate and the concreted beam and kept in that position for 30 mins to allow the adhesive to solidify. The beam was then returned to its previous position, the steel plates on the edges were removed, and the press tool was placed on the top and left for 24 hours to complete the cure of the adhesive.

Table 4 gives the beam numbers, the type of FRP, the type of adhesive, the concrete surface conditions, and the adhesive thickness.

2.2. Analyzing the Model of an RC Beam Strengthened with FRP by ANSYS[®] WB

The numerical analysis was carried out by the ANSYS WB program, which performs computations for the three-dimensional finite element programs [29]. In ANSYS, a fracture model developed by William-Warneke has been used as a source of multi-axis stress for concrete material models [30]. Again, the Newton-Raphson method [31] has been used to analyze the nonlinear behavior in this program [31]. In this

TABLE 2 Dimensions and Material Properties of FRP

FRP type	Density (N/m ³)	Width (mm)	Strain at break (min. value)	Tensile strength, f_{tu} (N/mm ²)	E-modulus E_f (N/mm ²)
		Thickness (mm)			
Sika CarboDur S1012	16000	100 1.2	>1.70%	35	165000

TABLE 3 Mechanical Properties of Adhesive Material Types

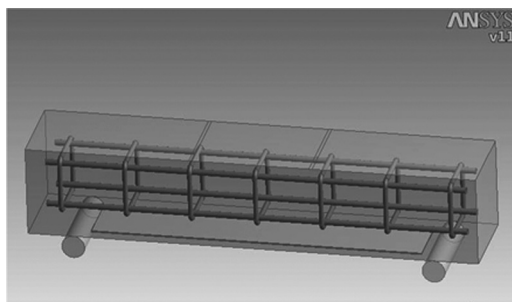
Adhesive type	Chemical base	Density (N/m ³)	Compressive strength (N/mm ²)	E-modulus (N/mm ²) Compressive/Tensile	Tensile strength (N/mm ²)	Bond strength (N/mm ²)
Sikadur-30	Epoxy resins	16500	70–80 (after 7 days)	9600/11200	24–27 (after 7 days)	>4 (after 7 days)
Sikadur-52	Low viscosity injection resins	10850	53 (after 10 days)	–	25 (after 10 days)	>4 (after 7 days)

TABLE 4 Material and Application Properties of Test Specimens

Beam no	FRP type	Adhesive type	FRP length (mm)	Concrete surface in application	Adhesive thickness (mm)
B01	Sika [®] CarboDur [®] S1012	Sikadur [®] -30	550	dry	<1
B02	Sika [®] CarboDur [®] S1012	Sikadur [®] -30	550	dry	1
B03	Sika [®] CarboDur [®] S1012	Sikadur [®] -30	550	dry	2
B04	Sika [®] CarboDur [®] S1012	Sikadur [®] -52	550	dry	1
B05	Sika [®] CarboDur [®] S1012	Sikadur [®] -52	550	dry	2
B06	Sika [®] CarboDur [®] S1012	Sikadur [®] -52	550	dry	4
B07	Sika [®] CarboDur [®] S1012	Sikadur [®] -30	550	dry	4
B08	Sika [®] CarboDur [®] S1012	Sikadur [®] -52	550	dry	4
B09	Sika [®] CarboDur [®] S1012	Sikadur [®] -30	550	dry	4
B10	Sika [®] CarboDur [®] S1012	Sikadur [®] -30	550	moistured	4
B11	Sika [®] CarboDur [®] S1012	Sikadur [®] -30	550	moistured	4
B12	Sika [®] CarboDur [®] S1012	Sikadur [®] -30	550	moistured	2
B13	Sika [®] CarboDur [®] S1012	Sikadur [®] -30	550	moistured	1
B14	Sika [®] CarboDur [®] S1012	Sikadur [®] -30	550	moistured	<1
B15	Control beam (RC beam)				

section, computer modelling of the test specimens and its finite element analyses are given. Material properties of the concrete, steel, and FRP specimens used in the numerical analyses replicate the features of the test specimens. The model of a RC beam strengthened with FRP prepared using ANSYS (Canonsburg, PA, USA) is displayed in Fig. 3.

In the program, solid modelling was performed for each type of material. The list of materials consisted of concrete, steel, support, FRP, and the adhesives (Fig. 4). Since modelling of steel is not available in ANSYS, longitudinal and horizontal steel re-bars were modeled in Solidworks 3D-solid drawing software (Solidworks Corp., Concord, MA, USA), whose models were then transferred into ANSYS environment.

**FIGURE 3** Finite element model in software.

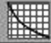
Concrete		Structural Steel	
<input type="checkbox"/> Structural Add/Remove Properties		<input type="checkbox"/> Structural Add/Remove Properties	
<input type="checkbox"/> Young's Modulus	32000 MPa	<input type="checkbox"/> Young's Modulus	2e+005 MPa
<input type="checkbox"/> Poisson's Ratio	0.2	<input type="checkbox"/> Poisson's Ratio	0.3
<input type="checkbox"/> Density	2.4e-006kg/mm ³	<input type="checkbox"/> Density	7.85e-006kg/mm ³
<input type="checkbox"/> Tensile Ultimate Strength	2.9 MPa	<input type="checkbox"/> Termal Expansion	1.2e-005 1/°C
<input type="checkbox"/> Compressive Ultimate Strng.	30 MPa	<input type="checkbox"/> Tensile Yield Strength	420 MPa
Multilinear Isotropic Hardening 		<input type="checkbox"/> Tensile Ultimate Strength	500 MPa
FRP_SikaCarbodur1012		Adhesive	
<input type="checkbox"/> Structural Add/Remove Properties		<input type="checkbox"/> Structural Add/Remove Properties	
<input type="checkbox"/> Young's Modulus	1.65e+005 MPa	<input type="checkbox"/> Young's Modulus	11200 MPa
<input type="checkbox"/> Poisson's Ratio	0.2	<input type="checkbox"/> Poisson's Ratio	0.22
<input type="checkbox"/> Density	1.6e-006kg/mm ³	<input type="checkbox"/> Density	1.65e-006kg/mm ³
<input type="checkbox"/> Compressive Yield Strength	75 MPa	<input type="checkbox"/> Tensile Ultimate Strength	25 MPa
<input type="checkbox"/> Tensile Ultimate Strength	35 MPa	<input type="checkbox"/> Compressive Ultimate Strng.	75 MPa

FIGURE 4 Material properties of composite model (for C30 concrete strength class and Sikadur-30).

In order to simulate the loading in the testing set up, analyses were conducted by applying the load over the beam onto a $5 \times 150 \text{ mm}^2$ area in ANSYS. In addition, the dimensional and material properties of the supports in the testing setup were made with the same modeling in ANSYS. In order to obtain the actual behaviour of the beam element the reinforced concrete beam model prepared in ANSYS is divided into a finite element mesh before the nonlinear analysis. The steel and concrete adherence effect and degrees of freedom of the supports are taken into account in the software analysis.

3. RESULTS AND DISCUSSION

3.1. The Results Obtained in the Experimental Study

As mentioned in the previous section, the specimen was placed in the experimental setup, the LVDT was fixed in midspan of the beam,

and then the computer-controlled experimental setup was ready. Deflections of beams depending on the load were measured by the test program interface screen, and the load-deflection results were obtained thereby. The experimental results for the tested models, namely, the load bearing capacity and maximum deflection values, were obtained and are exhibited in Table 5. Comparison of strength and deflection values of the beams is given in Table 6. The strengthened beams failed in two modes: (i) debonding failure and (ii) flexural failure. Flexural cracks were observed to be uniformly distributed within the FRP-bond zone on the tension face (Fig. 5a). The cracks were narrower in the strengthened beams in comparison with those observed in the control beam due to the presence of the FRP at the concrete surface. During debonding failure, the shear stress concentration around the flexural or shear crack opening displacements within the shear span may also lead to local debonding of the FRP along the concrete-FRP interface (Fig. 5b).

As a result of the tests conducted under laboratory conditions, the effects of shear/bending cracks and plate end interfacial debonding of FRP were obtained. Deflections at the beginning of the loading were very small. Following the first cracks formed in the tension face of the specimen, an increasing trend in the deflection values was observed. After the tests were conducted, the beams were examined and, as expected on the tension face, bending and shear behavior in the cracks

TABLE 5 Loads and Deflections at the Load Bearing Capacity of the Tested Beams

Beam no	Load when FRP applied (kN)	Ultimate load (kN)	Mid-span deflection δ (mm)	Failure mode
B01	–	191.4	2.83	Debonding
B02	–	194.1	2.77	Flexural
B03	–	197.2	2.65	Flexural
B04	–	194.0	2.67	Debonding
B05	–	194.4	2.74	Flexural
B06	–	197.2	2.56	Flexural
B07	–	211.0	2.38	Flexural
B08	–	206.9	2.59	Flexural
B09	–	199.7	2.51	Flexural
B10	–	199.6	2.71	Flexural
B11	–	174.0	2.75	Flexural
B12	–	179.6	2.94	Flexural
B13	–	203.1	2.39	Debonding
B14	–	207.2	2.44	Flexural
B15 (control beam)		62.4	5.16	Flexural

TABLE 6 Comparison of Strength and Deflection Values of Test Specimens

Adhesive thickness	Condition of concrete surface						Adhesive type	
	Strength ratio	Deflection ratio	Test specimen	Strength ratio	Deflection ratio	Test specimen	Strength ratio	Deflection ratio
*B15	1.00	1.00	B15	1.00	1.00	B15	1.00	1.00
B01	3.15	0.55	**B10	3.27	0.52	***B06	3.18	0.50
B02	3.20	0.53	B09	3.28	0.48	B09	3.28	0.48
B03	3.24	0.51						
B09	3.28	0.49						
*B15: control beam, B01 < 1, B02:1, B03:2, B09:4 (mm)			**B10: moistened, B09: dry (surface)			***B06: Sikadur52/B09: Sikadur30		

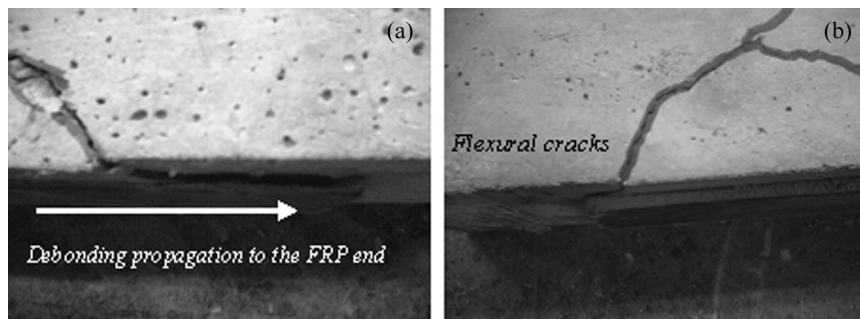


FIGURE 5 Failure types: (a) debonding failure (beam B13); (b) fail to flexure (beam B07).

were observed. Formation of shear cracks in the plate end occurred and debonding of the plate end in almost all of the specimens was also observed. The low values of bending deformations were remarkable. In the end, the mid-plate had not ruptured or fractured. It has been concluded that increasing the thickness of the adhesive reduces the vertical displacements.

3.2. The Results Obtained in the Numerical Analysis

The main objective of the computer model was to predict accurately the effects of strengthening with FRP on the parameters of the RC beams. Reinforced concrete beams used in the experimental study were modeled and analyzed in ANSYS and the shear and normal stress values in the adhesive-concrete and adhesive-FRP interfaces were obtained. The analyses are performed according to adhesive type, adhesive thickness and the concrete surface conditions, thus allowing comparison of the graphs. Sikadur-30 and Sikadur-52 were used as the adhesive and the adhesive thicknesses were chosen to be less than 1 mm, and precisely 1, 2, and 4 mm, respectively. The analyses were conducted by assuming the utilization of adhesive materials with non-linear or inelastic shear behaviour as the main mechanism of stress transfer between the RC beam and the FRP strip, and the stress values were determined in this manner.

3.2.1. Effects of the Adhesive Layer Thickness with Respect to the Stress

In such cases, the thickness of the adhesive layer was assumed to be 2 mm, a value similar to the mean values reported for the remaining

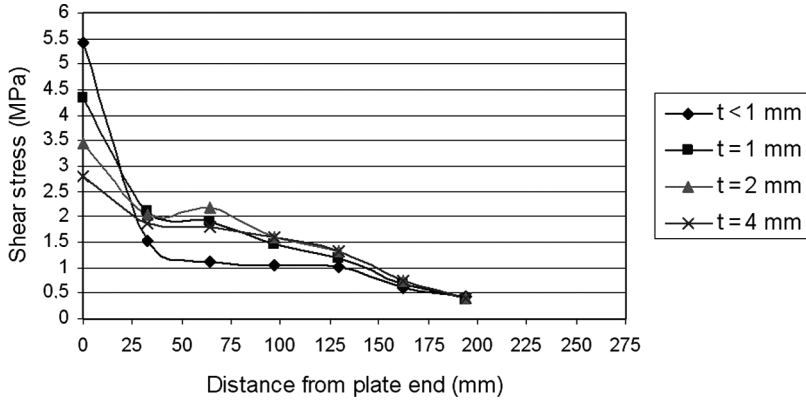


FIGURE 6 Shear stresses according to adhesive thicknesses.

beams with pultruded plates (averaging 1.88 mm from 32 tests) [32, 33, 34]. For the beams B01, B02, B03, and B09, all the parameters were kept constant throughout the experiment except for the thickness of the adhesive layer. After the beams were subjected to loading, shear and normal stress values for B01, B02, B03, and B09 specimens were obtained in ANSYS. The thicknesses of the implemented adhesives for the specimen were as follows; less than 1 mm for B01, and precisely 1, 2, and 4 mm for B02, B03, and B09, respectively. Stress values taken from the edge values were based on the FRP. Shear stresses (adhesive-to-FRP) are displayed in Fig. 6 and normal stresses in Fig. 7. Beam B01, with adhesive thickness of less than 1 mm, demonstrated higher stresses than those of the others at 0 distance from the plate end.

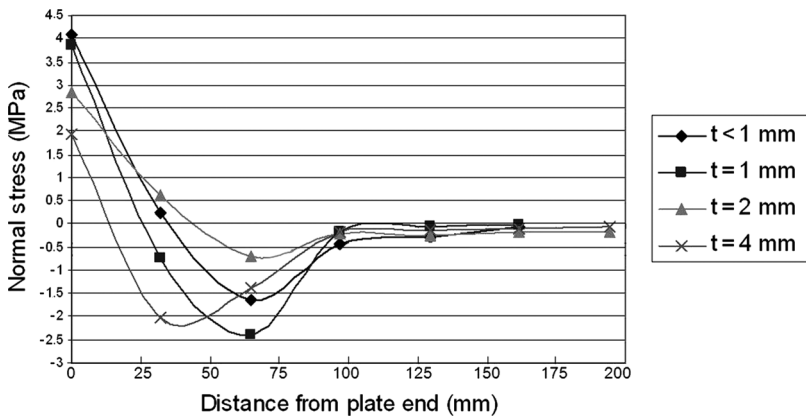


FIGURE 7 Normal stresses according to adhesive thicknesses.

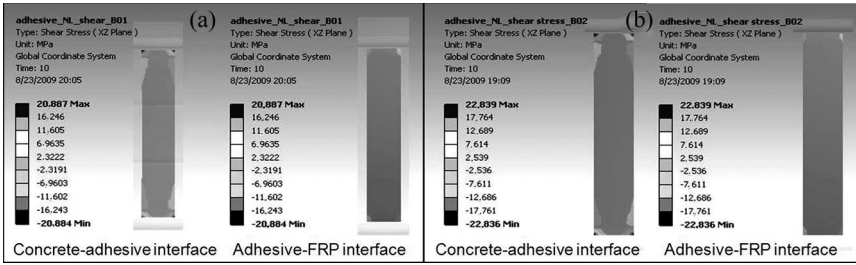


FIGURE 8 Contours of shear stress: (a) Beam B01; (b) Beam B02.

It has been clearly observed that increasing the thickness of the adhesive layer results in a significant reduction in peak interfacial stress values. Therefore, using thick adhesive layers is strongly recommended, especially in the edge zone of the FRP.

Shear stress contours have been plotted on a separate section on flexural stresses. The contours of B01, B02, B03, and B09 specimens for concrete-adhesive and adhesive-FRP interfaces are shown in Figs. 8 and 9.

Shear stress values at the FRP end are higher than the values at any other point. After the tests were carried out, debonding of the FRP ends occurred and the results of the analysis verified this debonding behavior. Shear stress values at the concrete-adhesive and adhesive-FRP interface exhibit variation nearby the FRP ends.

3.2.2. Effects of the Adhesive Layer Type with Respect to the Stress

Using Sikadur-30 and Sikadur-52 as the adhesives, the shear stresses (adhesive-to-FRP) for B03 and B05 specimens were obtained by ANSYS WB. Sikadur-30 in beam B03 and Sikadur-52 in beam B05 were used. Figure 10 shows the effects of the type of adhesive

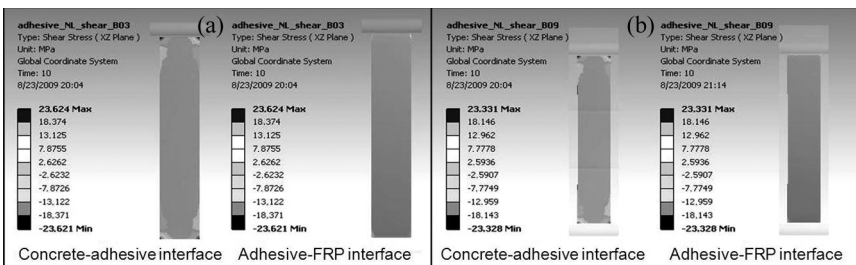


FIGURE 9 Contours of shear stress: (a) Beam B03; (b) Beam B09.

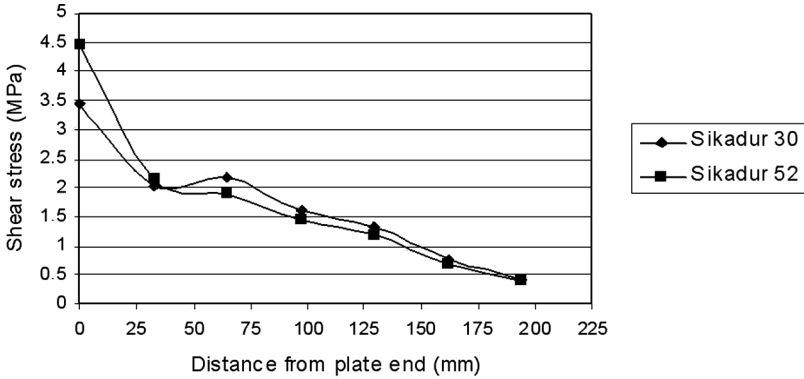


FIGURE 10 Shear stresses according to adhesive types.

layer on the interfacial stresses. Stress values were taken from the edge zones depending on the length of the FRP.

As shown in Fig. 10, stress values do not significantly vary with the adhesive type. In addition, the differences in deflection and the load bearing capacity for each adhesive type were not significant according to the experimental study. However, the relatively easy application of Sikadur-30 can be accepted as an advantage over Sikadur-52. Shear stresses decreased continuously from the FRP end points until the middle of the beam (distance from plate end: 200 mm) Moreover, the peak values of shear stresses can be seen in the neighbourhood of the FRP ends. Normal stress values are given in Fig. 11.

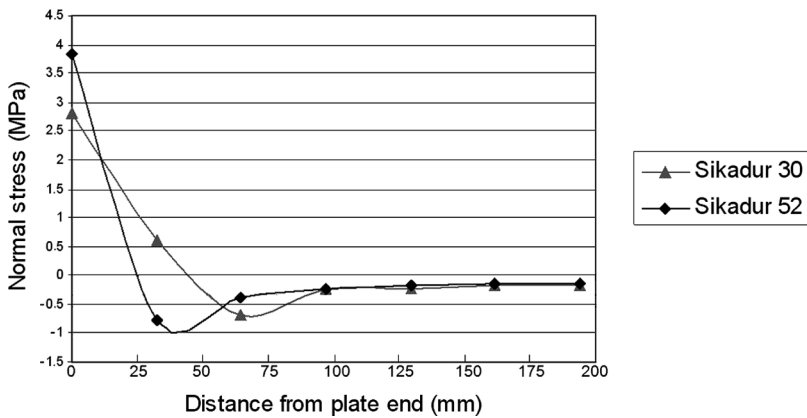


FIGURE 11 Normal stresses according to adhesive types.

From Fig. 11, it can be seen that the normal stress values were not considerably affected by the selection of adhesive type, either. Similarly, the peak values of normal stress were in the vicinity of the FRP ends.

3.2.3. Effect of the Concrete Surface Conditions with Respect to the Stress

The analysis was performed and shear stresses were obtained through an adhesive layer by taking the dryness/moisture conditions of the concrete surface into account. Material properties of B09 and B10 specimens used in tests were first simulated in the computer environment and then appropriate values for shear and normal stresses were assigned. The concrete surface of B09 was dry whereas that of B10 was moist at the moment of FRP application. Shear and normal stresses are given in Figs. 12 and 13, respectively.

Shear and normal stress values of B10 specimen were larger than those of B09 at 0 distance from the plate end, whereas the maximum deflection of B09 was less than B10 according to the experimental results. Decreasing shear stresses at the middle of the beam (distance from plate end: 200 mm) and the occurrence of shear stress peak values the FRP plate end are in accordance. This implies that applying FRP to a dry concrete surface is preferable to a moist surface.

3.2.4. Effect of Stress Transfer Characteristics at the Interface with Respect to the Stress

The analyses were performed based on the usage of adhesive materials with non-linear and inelastic shear behaviour between the RC

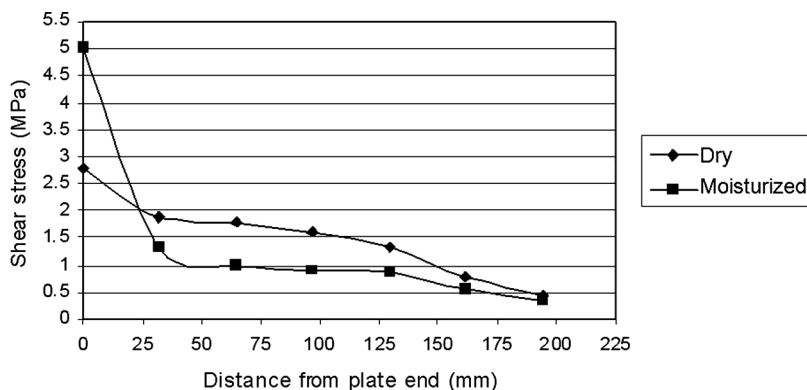


FIGURE 12 Shear stresses according to concrete surface conditions.

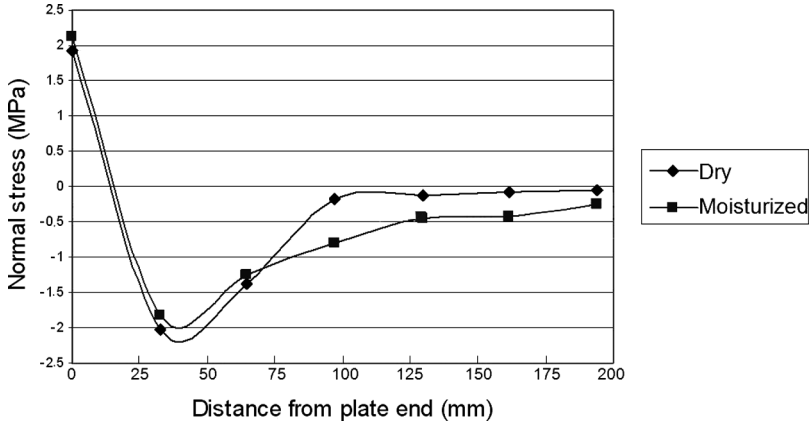


FIGURE 13 Normal stresses according to concrete surface conditions.

beam and FRP. This approach was developed by Rabinovitch [16]. Types of stress transfer were non-linear elastic (NL), linear elastic (L), and linear elastic-perfectly plastic (EP). Comparisons of the results are given in Figs. 14 and 15 for various types of stress transfer.

As shown in Fig. 14, the analysis results were evaluated based on the linear, nonlinear, and elasto-plastic behaviour of the adhesives. The shear stresses obtained in nonlinear cases had higher values than other cases. The elasto-plastic case produced the lowest shear stress values. Although the normal stress values in the vicinity of the FRP ends for the linear case is higher compared to the other cases, normal

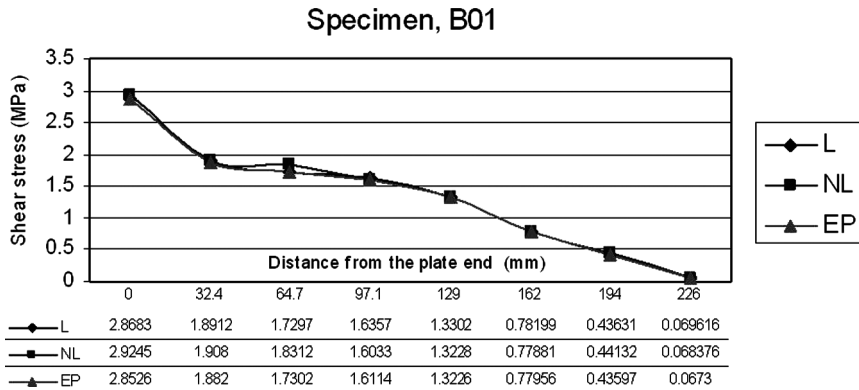


FIGURE 14 Shear stresses for various adhesives (L: linear, NL: nonlinear elastic, EP: elasto-plastic).

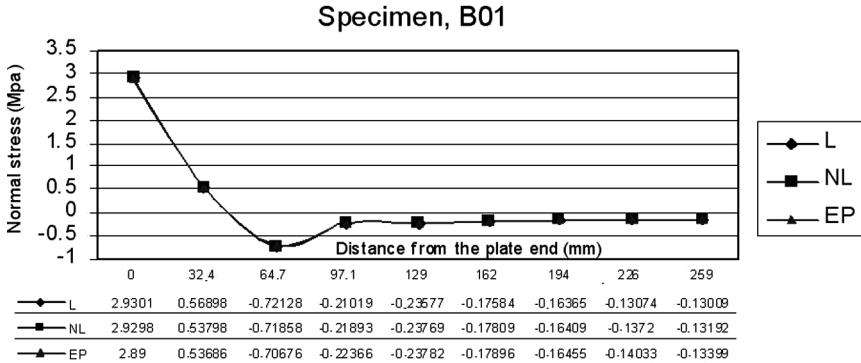


FIGURE 15 Normal stresses for various adhesives (L: linear, NL: nonlinear elastic, EP: elasto-plastic).

stresses in the mid-span of the adhesive layer in the linear case were lower in comparison to the cases of nonlinear elastic and elasto-plastic behaviour (Fig. 15). The contours of shear and normal stress of adhesive materials with linear, nonlinear, and elasto-plastic behavior are given in Figs. 16 and 17 for the B01 specimen.

The results have shown that the usage of elasto-plastic and linear adhesive materials reduces the interfacial shear stress, spreads them more uniformly, and cuts down the concentration of shear stress near the edge of the FRP.

Based on the above symptoms, it has been understood that the key to evaluating the interfacial stresses is to determine the stress concentration.

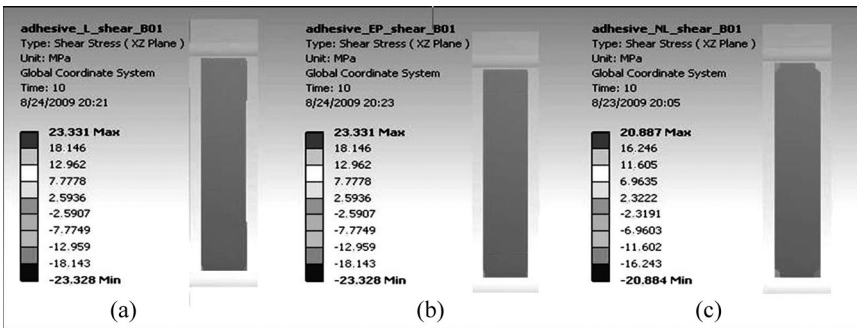


FIGURE 16 Contours of shear stress for B01: (a) linear; (b) elasto-plastic; (c) nonlinear.

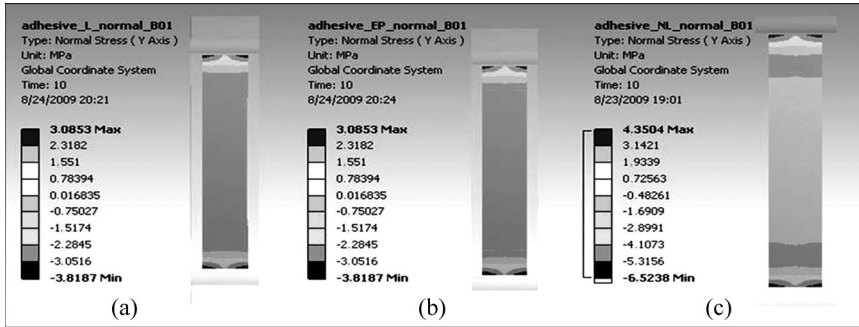


FIGURE 17 Contours of normal stress for B01: (a) linear; (b) elasto-plastic; (c) nonlinear.

4. CONCLUSIONS

There are many existing methods available for preserving, repairing, and strengthening building structures to address the effects of earthquakes in civil engineering literature. Using fibre-reinforced plastic (FRP) laminates as a strengthening method has turned out to be a quick and economical method in recent years. In this study, the behaviour of reinforced concrete beams strengthened with FRP and subjected to a two-point load has been presented. Next, the numerical analyses were performed to determine the effects of various parameters on the interfacial stresses of reinforced concrete (RC) beam strengthened with FRP. At this stage, the determination of interfacial stresses in the adhesive layer has been extensively analyzed for the beams tested in the experimental program and finite element modeling. The results of finite element (FE) analysis have been shown to be in close agreement with the corresponding experimental study which demonstrates the correctness and accuracy of the FE analyses. The main conclusion that can be drawn from the present study is that the above-mentioned parameters affected the concentration of interfacial shear and normal stresses in FRP, as well as load-bearing capacities of the beams and debonding at the FRP end. Furthermore, stress transfer characteristics have a significant effect on the adhesion behaviour of epoxy-bonded specimens.

Within the indicated scope of investigation, the particular conclusions derived from this study could be summarized as follows:

1. It has been concluded by our laboratory experiments that the observed deflections on FRP-applied reference beams have been

reduced by 50% and the load-bearing capacity has increased by three times compared to the regular reference beam behaviors. The low thickness of the adhesives that have been used to adhere FRP to the reference beams, which is less than 1 mm, has also singlehandedly decreased deflection of the examined reference beam by 9%. Therefore, the amount of FRP used as well as the adhesive thickness applied should also be taken into the account in order to determine the precise load-bearing capacity of the components during the design procedure.

2. Increasing the thickness of the adhesives used in our experiments has resulted in a reduction of the normal and shear stresses. Even though the thicknesses of adhesives are very low, it has been determined by our experiments that they should be taken into account in the engineering applications and it has been recommended that higher thicknesses should be preferred.
3. The surface of the concrete is highly critical terms of the bonding forces between the adhesives and the concrete. As a result of comparing different concrete surfaces, it has been determined that the moist surface possessed 4% less load-bearing capacity and 8% higher deflection than the dry surface did. It has been concluded that the concrete surface is not only important for practical purposes in real life applications but it should also be incorporated as a variable for the mathematical model.
4. As we compare two different types of adhesives (Sikadur 30 and Sikadur 52) for their effects on load-bearing capacities and deflections, differences of 1.2% and 4% have been observed, respectively. Since there is no discernible difference between two adhesives in terms of load-bearing and deflection capacity, no recommendation has been made regarding the types of the adhesives.
5. As the stress between the concrete surface and the adhesive exceeds the bonding force between them a separation emerges at the FRP ends. The stress contours of the reinforced concrete beams with FRP, which are generated by the numerical analysis, identify the plate ends as the most critical area.
6. As a result of conducting separate analyses for the linear, non-linear, and elastoplastic stress transfers from the adhesive to the plate and the concrete, large shear stress values during nonlinear stress transfers and lower shear stress values in elastoplastic stress transfer situations have been observed. For the adhesives, the elastoplastic stress transfer assumption that our laboratory experiments were based on has been determined to provide the closest results.

Based on the results obtained from experimental and finite element analysis, a number of recommendations for future research and application purposes are listed below:

1. It is necessary to study the behaviour of flexural strengthening of reinforced concrete (RC) beams under cyclic loads.
2. After the reinforced concrete (RC) beams are strengthened with FRP under static and dynamic loads, flexural behaviour of the beams should be investigated.
3. In addition to the bending effect, further examinations are needed for FRP plated RC beams considering the influence of shear deformation.
4. The influence of concrete surface conditions on the strengthened beams has been added to the current analytical deformation expressions. Afterwards, revised analytical equations have been obtained to determine load carrying capacity.
5. The numerical calculations of the strengthened reinforced concrete (RC) beams should be carried out to avoid shear force effect on failure, so that the shear capacity of the reinforced concrete (RC) beams can be obtained sufficiently.

ACKNOWLEDGMENTS

Istanbul University Scientific Research Projects Unit (Project No. T-2145) provided the financial support for this work. The authors wish to thank the Construction Materials Laboratory of Civil Engineering Department and the I.U. Scientific Research Projects Unit.

REFERENCES

- [1] ACI Committee 440, Report on fiber reinforced plastic reinforcement for concrete structures (ACI 440R-96), American Concrete Institute, Farmington Hills, p. 68, (Reapproved in 2002).
- [2] Fukuyama, H., Nakai, H., Tanigaki, M., and Uomoto, T., *Proceedings of the Third Symposium on Non-Metallic (FRP) Reinforcement for Concrete Structures*, (Japan, 1997), pp. 605–612.
- [3] Dong, Y., Zhao, M., and Ansari, F., *Proceedings of the Third International Conference on Composites in Infrastructure -ICCI'02* (San Francisco, California, 2002), pp. 51–65.
- [4] Ye, J. Q., *Cement Concrete Comp.* **23**, 411–417 (2001).
- [5] Wang, Y. C., Lee, M. G., and Chen, B. C., *Compos. Struct.* **81**, 491–498 (2007).
- [6] Casas, J. R. and Pascual, J., *Constr. Build. Mater.* **21**, 1940–1949 (2007).
- [7] Rougier, V. C. and Luccioni, B. M., *Eng. Struct.* **29**, 1664–1675 (2007).

- [8] De Lorenzis, L., Teng, J. G., and Zhang, L., *Int. J. Solids Struct.* **43**, 7501–7517 (2006).
- [9] Wang, J., *Int. J. Solids Struct.* **43**, 6649–6664 (2006).
- [10] Lee, H. K. and Hausmann, L. R., *Compos. Struct.* **63**, 201–209 (2004).
- [11] Wu, Z. J. and Davies, J. M., *Compos. Struct.* **62**, 139–143 (2003).
- [12] Ferreira, A. J. M., Camanho, P. P., Marques, A. T., and Fernandes, A. A., *Compos. Struct.* **53**, 107–116 (2001).
- [13] Yang, J., Ye, J., and Niu, Z., *Eng. Struct.* **30**, 533–545 (2008).
- [14] Rougier, V. C. and Luccioni, B. M., *Eng. Struct.* **29**, 1664–1675 (2007).
- [15] Gheorghiu, C., Labossiere, P., and Proulx, J., *Constr. Build. Mater.* **21**, 756–763 (2007).
- [16] Rabinovitch, O., *J. Struct. Eng.- ASCE* **131**, 1580–1592 (2005).
- [17] Masoud, S. and Soudki, K., *Cement Concrete Comp.* **28**, 969–977 (2006).
- [18] Teng, J. G., Yuan, H., and Chen, J. F., *Int. J. Solids Struct.* **43**, 5750–5778 (2005).
- [19] Gao, B., Leung, K. Y., and Kim, J. K., *Eng. Struct.* **27**, 177–189 (2005).
- [20] Jianzhuang, X., Li, J., and Quanfan, Z., *Constr. Build. Mater.* **18**, 745–752 (2004).
- [21] Chen, J. F. and Teng, J. G., *Constr. Build. Mater.* **17**, 27–41 (2003).
- [22] Pesic, N. and Pilakoutas, K., *Compos. Part B-Eng.* **34**, 327–338 (2003).
- [23] Smith, S. T. and Teng, J. G., *Eng. Struct.* **23**, 857–871 (2001).
- [24] Khalifa, A. and Nanni, A., *Cement Concrete Comp.* **22**, 165–174 (2000).
- [25] Alsayed, S. H., *Cement Concrete Comp.* **20**, 1–11 (1998).
- [26] Tounsi, A. and Benyoucef, S., *Int. J. Adhes. Adhes.* **27**, 207–215 (2007).
- [27] Eurocode 2, Design of concrete structures, BSEN 1992-1-1: 2004, British Standards Institution, United Kingdom.
- [28] Smith, S. T. and Teng, J. G., *Eng. Struct.* **24**, 397–417 (2002).
- [29] Moaveni, S., *Finite Element Analysis-Theory and Applications with ANSYS*, (Prentice Hall Inc., New Jersey, 1999), 10th Ed., pp. 527.
- [30] William, K. J. and Warnke, E. P., IABSE, Report No. 19, (Bergamo, Zurich, Switzerland 1974), pp. 1–30.
- [31] Ypma, T. J., *SIAM Review* **37**, 531–535 (1995).
- [32] Oehlers, D. J. and Ali, M., *Mag. Concrete Res.* **50**, 91–92 (1998).
- [33] Swamy, R. N., Jones, R., and Bloxham, J. W., *Struct. Eng.* **65A**, 59–68 (1987).
- [34] Quantrill, R. J., Hollaway, L. C., and Thorne, A. M., *Mag. Concrete Res.* **48**, 343–351 (1996).